Analytica Chimica Acta 723 (2012) 94–100

Contents lists available at SciVerse ScienceDirect

Analytica Chimica Acta

journal homepage: www.elsevier.com/locate/aca

# Glucose biosensor based on three dimensional ordered macroporous self-doped polyaniline/Prussian blue bicomponent film

Xiaojun Chen[a,b,*], Zixuan Chen[a], Rong Tian[a], Wei Yan[c], Cheng Yao[a]

[a] College of Sciences, Nanjing University of Technology, Nanjing 210009, PR China
[b] State Key Laboratory of Materials-Oriented Chemical Engineering, Nanjing University of Technology, Nanjing 210009, PR China
[c] Nano Science and Technology Research Center, Shanghai University, Shanghai 200444, PR China

ARTICLE INFO

*Article history:*
Received 19 December 2011
Received in revised form 13 February 2012
Accepted 15 February 2012
Available online 24 February 2012

*Keywords:*
Three dimensional ordered macroporous
Self-doped polyaniline
Prussian blue
Glucose oxidase
Biosensor

ABSTRACT

In this paper, a three dimensional ordered macroporous self-doped polyaniline/Prussian blue (3DOM SPAN/PB) bicomponent film was fabricated via the inverted crystal template technique using step-by-step electrodeposition. In this bicomponent film, PB not only acted as a redox mediator, but also presented increased stability in neutral or weak alkaline solution by the protection of SPAN layer on the top. A novel glucose biosensor was fabricated based on the large active surface area and excellent conductivity possessed by the 3DOM SPAN/PB film. The applying experimental conditions of the glucose biosensor have been optimized. Under the optimal conditions, the biosensor showed a wide linear range over three orders of magnitude in glucose concentrations (from 2 to 1600 μM) and a low detection limit of 0.4 μM. Moreover, the biosensor exhibited short response time, high selectivity and excellent operation stability, which can be applied to detect the blood sugar in real samples without any pretreatment.



## 1. Introduction

Among enzyme-based electrochemical biosensors, the glucose biosensor is the most extensively studied for the clinical significance of controlling diabetes [1]. Compared with mono-enzymatic glucose oxidase (GOD) system, the bi-enzymatic GOD–peroxidase system can permit the electrochemical detection of glucose at substantially milder potential and effectively avoid the interference of the coexisting electroactive substances, such as ascorbic acid (AA), uric acid (UA) and acetaminophen (AP). Furthermore, the cascade scheme of the bi-enzymatic system, where an enzyme is catalytically linked to another enzyme, can produce signal amplification and therefore enhance biosensor efficiency [2]. Prussian blue (PB), ferric hexacyanoferrate, is commonly considered as an "artificial peroxidase" due to its high activity and selectivity toward the reduction of $H_2O_2$. It has been extensively used in the construction of bi-enzymatic glucose biosensors, resulting in improved signal-to-noise ratio [3]. However, low electrochemical stability of PB in neutral medium has restrained the further development of PB-based biosensors because the enzyme-catalyzed reactions involved in biosensors are usually operated in neutral buffer solution [4]. Incorporating PB into nanocomposites can greatly improved the stability of PB in neutral buffer solutions. Recently, an amperometric glucose micro-biosensor based on PB modified carbon fiber electrode has been prepared for physiological application [5]. Fu et al. developed an electrochemical glucose biosensor based on PB-carbon nanotubes hybrids, which exhibited two orders of linear range and rapid response rate [6]. Zhang et al. electrodeposited PB on a glassy carbon electrode modified by titanium dioxide-multiwall carbon nanotubes-chitosan ($TiO_2$-MWNTs-CS) composite, and then GOD and Au nanoparticles were adsorbed on the PB film, based on which a new glucose biosensor was prepared [7]. All of the above glucose biosensors showed enhanced sensitivity and stability in neutral medium.

Three-dimensional ordered macroporous (3DOM) films have attracted increasing attention in the development of electrochemical sensors due to their fascinating properties [8–10]. They can provide large active surface, which is promising to increase functional density and facilitate electron exchange, resulting in several orders of magnitude in electrochemical signals and thus the sensitivity of the fabricating devices [11]. Various materials such as metals, alloys, oxides and polymers can be electro-deposited in the interspaces of sacrificial templates composed of silica or latex spheres, which provide a useful approach for the preparation of 3DOM materials. The technique offers some advantages such as: thickness control through the amount of circulating charge, production of self supported layers and a wide choice of materials [12–16].

Herein, a 3DOM SPAN/PB bicomponent film modified Au electrode was prepared through electro-polymerization method using the ordered colloidal assembly of silica spheres as sacrificial

* Corresponding author at: College of Sciences, Nanjing University of Technology, Nanjing 210009, PR China. Tel.: +86 25 83587433; fax: +86 25 83587433.
*E-mail address:* chenxj_njut@126.com (X. Chen).

0003-2670/$ – see front matter © 2012 Elsevier B.V. All rights reserved.
doi:10.1016/j.aca.2012.02.032

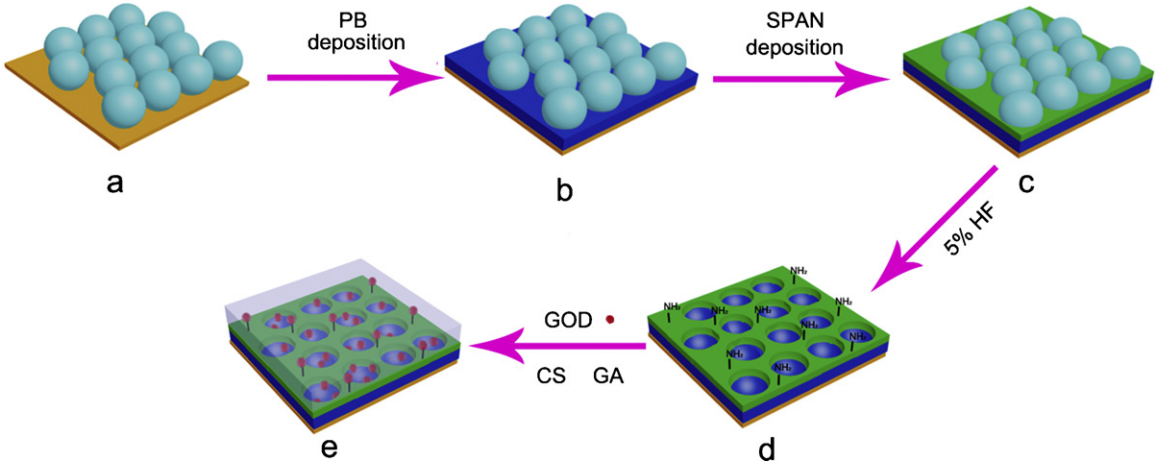


**Scheme 1.** Schematic illustration of the stepwise glucose biosensor fabrication.

template. After GOD was immobilized on the 3DOM SPAN/PB bicomponent film via covalent cross-linking among CS, SPAN and glutaraldehyde (GA), a novel glucose biosensor with high sensitivity was prepared. This 3DOM SPAN/PB bicomponent film brought three main advantages: (1) the interconnected 3DOM SPAN/PB bicomponent film had large surface area, which could increase the quantity of the immobilized GOD molecules for glucose sensing; (2) the SPAN component could maintain the electrochemical activity of the PB even in basic medium; (3) the SPAN component can improve the conductivity of 3DOM SPAN/PB film. In this paper, effects of electro-deposition charges of PB and SPAN, pH value, applied potential and temperature on current response of the glucose biosensor were optimized. The results showed that the biosensor exhibited good stability, high sensitivity, rapid response, good reproducibility, long-term stability and freedom of interference from other co-existing electro-active species. The biosensor can be used to determine the glucose concentration in human serum samples.

## 2. Experimental

### 2.1. Reagents

The monodispersed silica spheres with the diameter of 500 nm were obtained from Alfa Asear. Aniline (AN) was distilled twice under reduced pressure and stored in dark at low temperature before use. The supporting electrolyte phosphate buffer saline (PBS, 0.1 M) was prepared by mixing the stock solutions of $KH_2PO_4$ and $K_2HPO_4$, and adjusted to appropriate pH by adding 0.1 M KOH or $H_3PO_4$ solution. GOD (EC 1.1.3.4, 300 U $mg^{-1}$, from *Aspergillus niger*) was purchased from Sigma. Stock solution of 10 mg $mL^{-1}$ GOD was freshly prepared in pH 6.0 PBS. Chitosan (CS) was purchased from Aldrich. CS stocking solution was prepared by dissolving CS flakes in 1% acetic acid. GA (25 wt%) was supplied by Chengdu Kelong Chemical Reagents. $H_2O_2$ (30%, w/v solution) was obtained from Sinopharm Chemical Reagent Co. Ltd., and its accurate concentration was determined by titration with potassium permanganate. 3-Aminobenzenesulfonic acid (SAN) was purchased from TCI. Potassium ferricyanide ($K_3[Fe(CN)_6]$), potassium ferrocyanide ($K_4[Fe(CN)_6]$) and potassium chloride (KCl) were all purchased from Shanghai Linfeng Chemical Reagent Co. Ltd. Human serum samples were obtained from Institute of Dermatology, Chinese Academy of Medical Sciences and used as received. Glucose stock solution was allowed to mutarotate at room temperature overnight before use. Other reagents were of analytical grade and used without any further purification. All the solutions were prepared with double distilled water.

### 2.2. Instruments

All electrochemical experiments were performed using a CHI660D electrochemical workstation (Shanghai CH Instruments Co.) using a traditional three-electrode system. A twisted platinum wire and a saturated calomel electrode (SCE) were used as counter and reference electrode, respectively, and the 3DOM SPAN/PB film modified electrode ($\Phi$ = 3 mm) was used as working electrode. All potentials herein are referenced to the SCE. The sensor responses were measured as the difference between total and residual currents. The morphology and composition of the 3DOM SPAN/PB film were verified by scanning electron microscopy (SEM, LEO1530VP) and Fourier transform infrared spectroscopy (FTIR, Bruker model VECTOR22), respectively.

### 2.3. Fabrication of the glucose biosensor

The fabrication process of the biosensor is shown in Scheme 1. Preparation of the 3D silica close-packed colloidal crystal modified gold electrode with controlled area ($\Phi$ = 3 mm) was similar to that described in Ref. [17] (Scheme 1a). Then, SPAN/PB bicomponent was electrochemically deposited into the template interspaces step by step. Firstly, the 3D silica modified gold electrode was inserted into an aqueous mixture consisting of 2.5 mM $K_3Fe(CN)_6$, 2.5 mM $FeCl_3$, 0.1 M KCl and 0.1 M HCl, then a constant potential of −0.40 V was applied until the deposition charge was up to 0.75 mC (Scheme 1b). Subsequently, the PB-modified electrode was rinsed with PBS (pH 4.0) and immersed into a solution containing 0.1 M KCl + 0.1 M HCl for cyclic potential sweep in the potential region of 0.05 and 0.35 V at a scan rate of 50 mV $s^{-1}$, until a stable voltammetric response was obtained. After that, the electro-polymerization of SPAN was accomplished in a solution of 1.0 M HCl, 0.1 M SAN and 0.5 M AN by potentiostatic technique at a potential of 0.65 V until the charge reached 1.5 mC (Scheme 1c). After thoroughly rinsed with 1.0 M HCl, the resulting electrode was immersed into aqueous HF (5%) for 2 min to remove the silica template, and a single-layered 3DOM SPAN/PB inverse opal was formed (Scheme 1d). In a similar condition, 3DOM PB without the protection of SPAN was also prepared.

The glucose biosensor was fabricated as follows: firstly, 10 μL of CS stock solution was mixed with 10 μL of GOD stock solution and 5 μL of 2.5 wt% GA water solution. Then, 10 μL of the mixture was

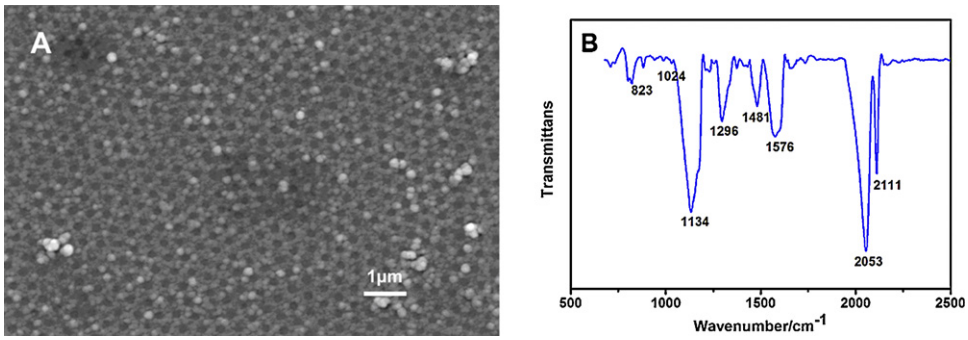


**Fig. 1.** (A) SEM image and (B) FTIR spectrum of 3DOM SPAN/PB bicomponent film modified electrode.

cast onto the 3DOM SPAN/PB film. The resulting CS–GOD/3DOM SPAN/PB was obtained after the electrode was dried in air at 4 °C for 12 h (Scheme 1e) and then immersed into a pH 6.0 PBS for 30 min to remove the redundant adsorbed GOD before use.

### 2.4. Electrochemical measurements

For steady-state amperometric experiments, the working potential was set at 0.0 V and the solution was stirred gently with a magnetic stirrer. The measurements of glucose concentration in serum samples were carried out by adding certain volume serum into the electrochemical cell with 10 mL PBS (pH 6.0) under stirring.

## 3. Results and discussion

### 3.1. Preparation of the 3DOM SPAN/PB film electrode

The electro-polymerization technique represents a good strategy to synthesize various inverse opals because the morphology and thickness can be controlled. Electro-polymerization technique also presents some additional advantages for synthesis, such as easily controllable reaction conditions including the applied potential or time, and molecular arrangement. Some studies showed that the construction of 3DOM materials using electro-polymerization was faster, simpler, and more energy efficient than traditional chemical methods [18–20]. To the best of our knowledge, there are no previous reports on the preparation of 3DOM SPAN/PB bicomponent film by this technique. The morphology of 3DOM SPAN/PB film was characterized by SEM, as shown in Fig. 1A. It was hexagonally close-packed, which indicated an inverse opal structure of a continuous 3DOM nature. The average diameter of the pores in this macroporous structure was about 250 nm and the average wall thickness of the pores was about 100 nm. The average distance between the pore centers was approximately 350 nm, which corresponded to a linear shrinkage of ca. 13% when compared to the original size of the colloidal templates (actually about 400 nm). This shrinkage value was similar to that theoretically expected, which assuming the isotropic shrinkage of sample was ca. 14% [21]. The lower degree of shrinkage probably owed to the well controlled electro-deposition which allowed the in situ formation of PB to start from the bottom of electrode and fill the interstices of template.

The amount of applied charge on electro-polymerization during deposition has great impact on the formation of the pores and the mechanical stability of 3DOM SPAN/PB bicomponent film. The deposition amount of PB was determined by the controlled charge in process of electro-deposition, which had been characterized by SEM images (not shown). When the controlled charge was less than 0.75 mC, only a few shapeless pores were observed. While some of the pores began to close when the charge was increased to 1.0 mC. If the charge was increased further, all the pores were closed. Moreover, the charge in the electro-deposition of SPAN was also optimized. When the charge was less than 1.5 mC, the PB film could not be protected by SPAN layer entirely, inducing the electrochemical signals of PB to decline continuously during cyclic voltammetry (CV) scans. When the charge exceeded 4.0 mC, too much SPAN was loaded on the electrode surface to make the mechanical stability of the SPAN film rather poor. With controlled charge increasing from 1.5 mC to 4.0 mC, the response current increased, while the noise and the response time increased too. Therefore, the controlled charges of 0.75 mC for PB and 1.5 mC for SPAN were chosen to obtain an ideal single-layered 3DOM structure similar to Fig. 1A.

Fig. 1B shows the FTIR spectrum of 3DOM SPAN/PB film. Two bands were observed at 2053 and 2111 $cm^{-1}$ which could be attributed to the C—N stretching region. The lower-wave-number band at 2053 $cm^{-1}$ could be assigned to the linear non-bridging mode of cyanide, indicating that the SPAN/PB bicomponent was mixture rather than compound. The higher-wave-number band at 2111 $cm^{-1}$ could be assigned to the end-on bridging mode of cyanide [22]. The characteristic bands of emeraldine salt form of SPAN at 1576 and 1481 $cm^{-1}$ could be assigned to C=C stretching mode of quinoid rings and benzenoid rings, respectively [23]. The C—N stretching of secondary aromatic amines (1296 $cm^{-1}$) and the aromatic C—H bending (1134 $cm^{-1}$) were also observed [24,25]. The bands at 1024 $cm^{-1}$ was attributed to the O=S=O stretching vibration. Moreover, the peak observed at 823 $cm^{-1}$ revealed the presence of 1,2,4-trisubstitution of aromatic ring [26]. These peaks were similar to our previous report, which proved the existence of SPAN in the 3DOM SPAN/PB structure [27].

### 3.2. Electrochemical characterization of the 3DOM SPAN/PB film electrode

The CV technique was used to characterize the electrochemical behavior of 3DOM SPAN/PB bicomponent film modified electrode, as shown in Fig. 2A. With scan rate increasing from 25 to 500 mV $s^{-1}$, the anodic and cathodic peak currents increased linearly with the square root of scan rate, indicating a diffusion-controlled process.

The electrochemical behavior and stability of 3DOM SPAN/PB bicomponent film to pH changes were also studied. It is well known that PB is unstable and dissolvable in neutral and alkaline solution because the hydroxyl ions are able to break the Fe—CN—Fe bond and dissolve the PB, which suggests a limited use of PB modified electrode in alkaline solution [28,29]. On the other hand, pure polyaniline (PANI) is electro-active only when pH is lower than 4.0, while the electro-activity of copolymer SPAN is greatly improved in neutral and alkaline solution, which has been proved in our previous work [27]. Fig. 2B shows respective responses of voltammetric peak current of 3DOM PB modified electrode (group b) and 3DOM SPAN/PB modified electrode (group a) upon the pH of buffer solution after 50 cycles scanning. For 3DOM PB modified electrode, the

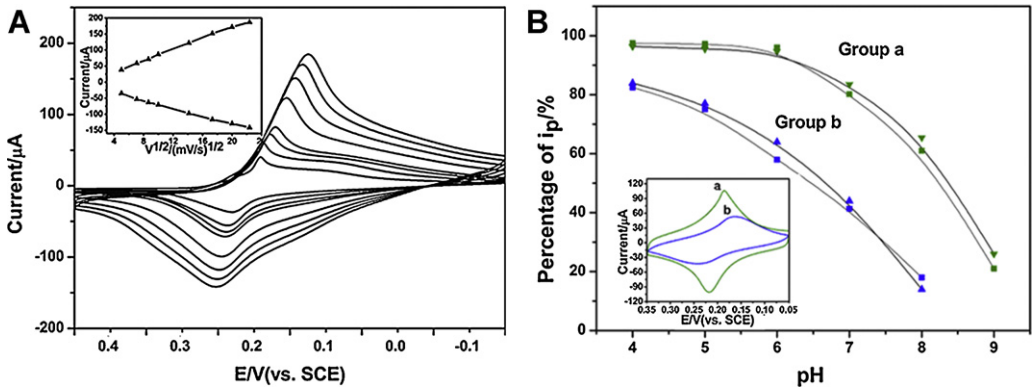


**Fig. 2.** (A) CVs of the 3DOM SPAN/PB bicomponent film modified electrode at 25, 50, 75, 100, 200, 300, 400, 500 mV $s^{-1}$ (from internal to external) in 0.1 M pH 6.0 PBS. The inset shows the plots of the peak current vs. $v^{1/2}$. (B) CV peak currents of 3DOM SPAN/PB bicomponent (group a) and 3DOM PB (group b) dependent on pH, inset is the CV curves at pH 6.0.

efficiency decreased about 60% when the pH increased from 4.0 to 6.0, and the redox currents decreased with the increase of pH and disappeared at pH 8.0, indicating the inactivation or dissolution of PB. While it could be observed that the 3DOM SPAN/PB modified electrode became more stable along with the increasing pH values. As a result, the amperometric efficiency would be maintained 95% at pH 6.0, 88% at pH 7.0 and 65% at pH 8.0, which was much better than previous reported results [30]. Such excellent electroactivity of the 3DOM SPAN/PB bicomponent film in the near neutral solutions might be attributed to the good electro-stability of PB protected by SPAN and the good conductivity of SPAN.

### 3.3. Electrochemical performances of the modified electrodes

Fig. 3 displays the CV curves at different modified electrodes in pH 6.0 PBS. No obvious electrochemical signals could be obtained at a bare gold substrate because of lacking electron mediator (curve a). In contrast, after the substrate was modified with 3DOM PB, a pair of well-defined peaks could be observed (curve b), which was the characteristic of PB redox couple. Higher response current and smaller peak-to-peak separation ($\Delta E_p$) could be obtained after the 3DOM SPAN/PB modification (curve c). The doped —$SO_3H$ groups in SPAN layer could provide an acidic microenvironment for PB layer in neutral solution, which contributed PB to exhibit good electrochemical activity under the protection of SPAN layer. The

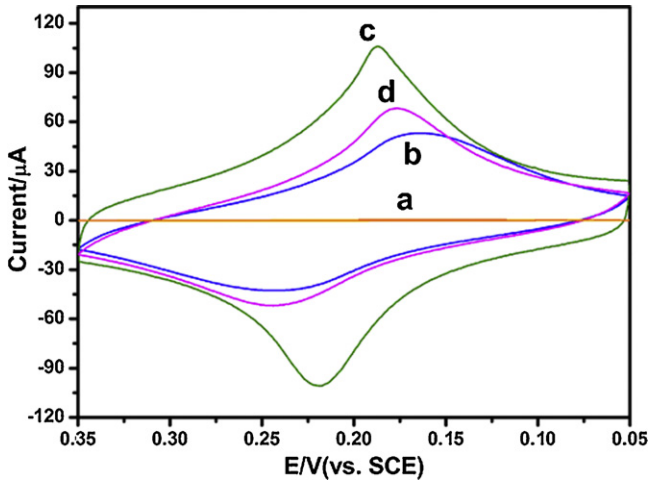


**Fig. 3.** CVs obtained at a scan rate of 50 mV $s^{-1}$ from different modified electrodes in pH 6.0 PBS. The bare gold substrate (a), 3DOM PB (b), 3DOM SPAN/PB (c) and CS–GOD/3DOM SPAN/PB (d).

combination of CS–GOD on 3DOM SPAN/PB film was accompanied with an obvious decrease of the peak currents and an increase in $\Delta E_p$ (curve d), which might be ascribed to the non-conductive GOD and CS obstructing electron transfer between 3DOM SPAN/PB and the surface of Au substrate.

### 3.4. Optimization of experimental parameters for glucose biosensor

In order to maximize the detection sensitivity of the proposed glucose biosensor, various conditions were optimized by single factor experiments, including the pH value of electrolyte, the working potential of chronoamperometry and the temperature.

It is of great importance to investigate the effect of pH value on the performance of biosensor, because the activity of immobilized GOD is pH dependent [31]. The change of chronoamperometric current with pH under 1.0 mM glucose is shown in Fig. 4A. The maximum response current of enzyme electrode appeared at pH 6.0, which indicated that the 3DOM SPAN/PB structure did not alter the optimum pH for the immobilized GOD [32]. Karyakin et al. found that the inactivation constant of PB was decreased almost 100 times when phosphate buffer was used as media solution [33]. Another interesting research found that a pair of well-defined and sharp peaks of PB mediator could be obtained in $K^+$ solution, which had been explained in terms of hydrated ionic radius and channel radius of the PB lattice [34]. Hence, in our experiment, the PBS (pH 6.0) composed of $KH_2PO_4$ and $K_2HPO_4$ was chosen as the optimal supporting electrolyte in consideration of the bioactivity of GOD and electro-activity of PB.

The choice of applied potential is fundamental to achieve the lowest detection limit and to avoid the electrochemical interfering species. The effect of applied potential on the enzyme electrode response showed that the sensitivity of enzyme electrode increased sharply with the applied potential decreasing from 0.20 to 0.0 V, as shown in Fig. 4B. At 0.0 V, sufficient current response was obtained, the background current was reduced and interference of other electro-active species could be avoided, therefore 0.0 V was selected as the applied potential in subsequent experiments.

The effect of temperature was also investigated in the range of 10–60 °C by steady-state amperometry at 0.0 V in PBS (pH 6.0) in the presence of 1.0 mM glucose. Before the amperometric detection, the biosensor was immersed into the buffer solution at different temperatures until thermal equilibrium. The result is shown in Fig. 4C. With an increasing temperature from 10 even to 50 °C, the activity of immobilized enzymes increased, leading to the increasing amperometric response. When the temperature was higher than 50 °C, the amperometric response decreased, owing

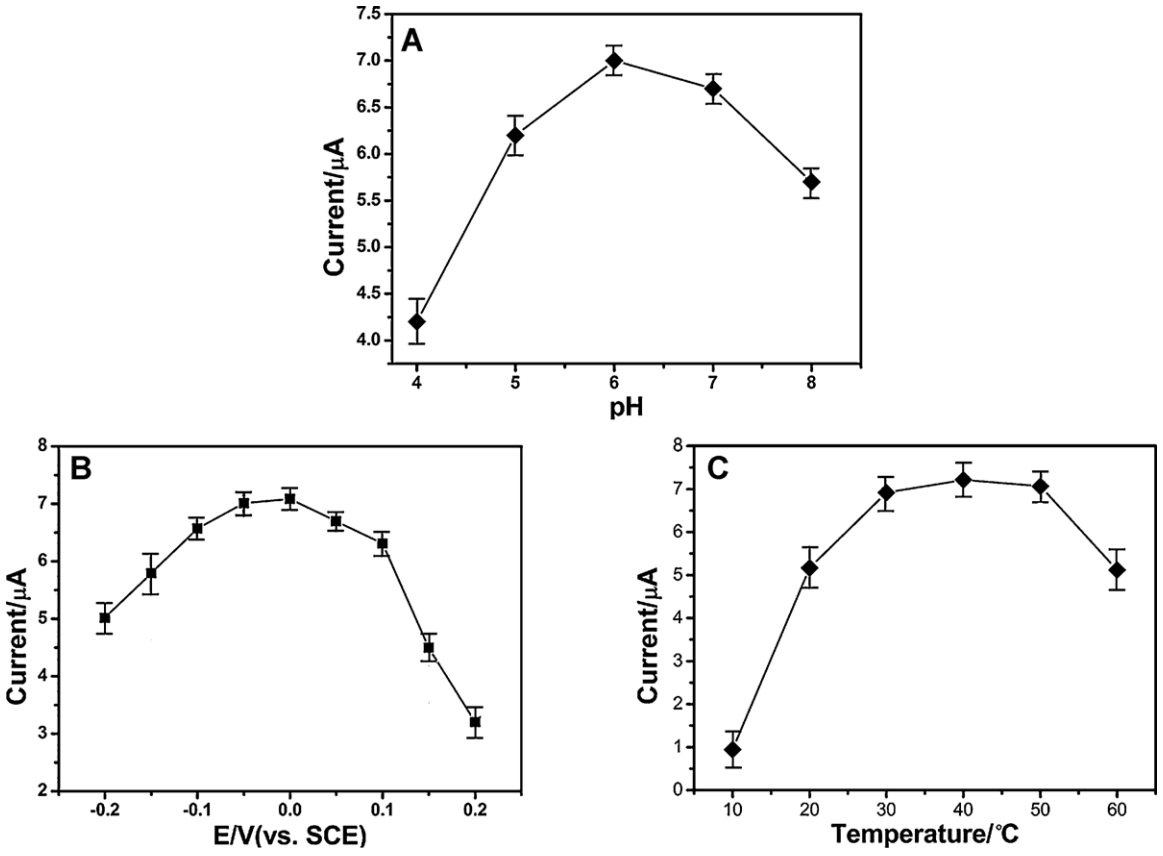


**Fig. 4.** Dependence of amperometric response of 1.0 mM glucose in 0.1 M PBS at CS–GOD/3DOM SPAN/PB modified electrode on the solution pH (A), working potential (B) and temperature (C).

to the denaturation of enzyme. As the optimum temperature of free GOD is around 30 °C [35], the good thermo-stability and activity at about 40–50 °C for the immobilized GOD may be due to the good microenvironment provided by CS matrix and 3DOM SPAN/PB structure. For practical convenience, all experiments were carried out at 35 °C, at which the response was 94% of the maximum.

### 3.5. The response characteristics of the glucose biosensor

#### 3.5.1. The response mechanism of the glucose biosensor

The mechanism involved in the detection of glucose with generation of $H_2O_2$ can be expressed as following. GOD catalyzes the oxidation of glucose in the presence of molecular oxygen to produce $H_2O_2$ according to Eq. (1), so the concentration of $H_2O_2$ is directly proportional to the concentration of the glucose. Therefore, the concentration of the glucose can be monitored indirectly during the course of the reaction.

$$\text{Glucose} + O_2 \xrightarrow{\text{GOD}} \text{Gluconolactone} + H_2O_2 \quad (1)$$

PB film can be reduced to the colorless form PW, as shown in Eqs. (2) and (3): where $Fe^{II}$ and $Fe^{III}$ correspond to different oxidation states of Fe atoms in the PB structure. PW can electrocatalytically reduce $H_2O_2$, acting as an electron transfer mediator between the substrate and $H_2O_2$ formed in the enzymatic reaction.

$$K_4Fe_4{}^{II}[Fe^{II}(CN)_6]_3(PW) + 2H_2O_2 \rightarrow Fe_4{}^{III}[Fe^{II}(CN)_6]_3(PB) + 4OH^- + 4K^+ \quad (2)$$

$$Fe_4{}^{III}[Fe^{II}(CN)_6]_3 + 4e^- + 4K^+ \rightarrow K_4Fe_4{}^{II}[Fe^{II}(CN)_6]_3 \quad (3)$$

The whole process is fast. With the series of reactions circulating continuously, an electric current response is induced and quantitatively detected on the modified electrode. Here we employed a 3DOM SPAN/PB bicomponent film to preserve the electro-activity of PB, and yield good electrocatalytic properties for reduction of $H_2O_2$.

#### 3.5.2. Amperometric response of the glucose biosensor

The typical current–time response for glucose detection is shown in Fig. 5. Upon successive injection of glucose into electrochemical cell with stirring under optimized conditions, the

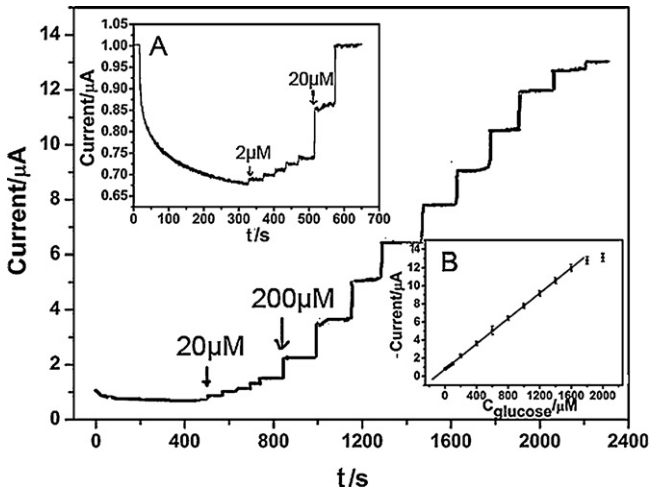


**Fig. 5.** Amperometric response of CS–GOD/3DOM SPAN/PB bicomponent film modified electrode to the successive addition of glucose at the applied potential of 0.0 V in 0.1 M PBS (pH 6.0). Inset (B) Lineweaver–Burk plot of the biosensor.

**Table 1**
Comparison of the analytical performances of different glucose biosensors.

| Electrode fabrication | Linear range | Detection limit (μM) | $K_m$ (mM) | Sensitivity (μA mM$^{-1}$ cm$^{-2}$) | Ref. |
|---|---|---|---|---|---|
| POPD/GOD-GA/PB/Au | 0.05–10 mM | 8 | 19.6 | – | [36] |
| GOD/PB/CS | 0.002–0.4 mM | 0.397 | 3.73 | – | [16] |
| PB/MWNTs/GCE | 0.5–8 mM | 12.7 | 18 | – | [37] |
| PB-GOD-Nafion/GCE | 0.15–2.5 mM | 30 | – | – | [38] |
| RuOX-PB/SPE | 0.3–20 mM | 40 | 130 | 6.2 | [39] |
| PB/MWNTs-GOx-CS-ICPTES/GCE | 0.025–1.3 mM | 7.5 | 2.75 | 15.2 | [20] |
| GOD/$SiO_2$/PB/Au | 0.01–5.8 mM | 0.94 | – | 26.6 | [23] |
| GOD-CS/$SiO_2$/PB/GCE | 0.05–26 mM | 8 | 3.2 | – | [40] |
| CS–GOD/3DOM SPAN/PB | 0.002–1.6 mM | 0.4 | 2.09 | 99.4 | This work |

amperometric response of the biosensor increased steeply and reached 95% of the steady-state current in less than 10 s, which implied that the biosensor's response was very fast. The linear response range of the biosensor to glucose concentration was from 2 to 1600 μM with a correlation coefficient of 0.99995 ($n$ = 21). The regression equation was expressed as $I$ (μA) = 0.769 + 7.02$C_{glucose}$ (mM), with the sensitivity of 99.4 μA mM$^{-1}$ cm$^{-2}$. Even at low concentration of glucose, obvious current response could be observed (inset A of Fig. 5). According to the linear equation, we could detect glucose concentration quantitatively. Higher glucose levels could be detected by an appropriate dilution with pH 6.0 PBS. The detection limit of this biosensor was estimated as 0.4 μM at a signal-to-noise ratio (S/N) of 3. The S/N and detection limit at the 3DOM SPAN/PB modified electrode could be greatly improved because it could supply much more active sites for the GOD immobilization and then the electrochemical reduction currents of $H_2O_2$ would be increased. The detection of low glucose level was very important for noninvasive measurements, because in such technologies sweat or tears was required to substitute for blood, in which the glucose concentration was about 100 times lower than that in blood [18]. Thus, highly sensitive glucose biosensor would have great potential in developing the noninvasive blood sugar measurement.

Once the concentration of glucose exceeded the linear range, the response current increased relaxedly and went stable at about 11.20 μA, showing the characteristics of Michaelis–Menten kinetics. The apparent Michaelis–Menten constant ($K_m$) could be obtained from the electrochemical version of Lineweaver–Burk equation: $1/I_{ss} = 1/I_{max} + K_m/(I_{max}C_{glucose})$, where $I_{ss}$ was the steady-state current after addition of the substrate, $C_{glucose}$ was the bulk concentration of the glucose, and $I_{max}$ was the maximum current measured under saturated conditions. $K_m$ could be obtained by analyzing the slope and intercept of the curve plotted from the reciprocals of steady-state current against glucose concentration which could be gained from inset B of Fig. 5, as determined to be 2.09 mM, illustrating the non-denaturating character of the enzyme-anchoring procedure. The small value of $K_m$ also indicated that the diffusion of substrate and product through the 3DOM SPAN/PB film was relatively easy, and the proposed enzyme biosensor had a high biological affinity toward glucose.

In order to assess the analytical performance of the proposed biosensor, the characteristics in terms of linear detection range, detection limit, sensitivity and $K_m$ were compared with earlier glucose biosensors based on PB composites, as presented in Table 1. Results showed the performance of proposed biosensor was better than the others, which might be attributed to the excellent conductivity and biocompatibility of 3DOM SPAN/PB bicomponent film. Meanwhile, the synergistic effect between SPAN and PB might give rise to the microenvironment to change enzyme and influence the intrinsic properties of enzyme.

### 3.5.3. Reproducibility and stability of the glucose biosensor

Reproducibility and stability are two important parameters for biosensors. The reproducibility of glucose biosensor in the online assays for 10 repetitive injections of 1.0 mM glucose in PBS was measured, and the relative standard deviation (RSD) was calculated to be 2.6%. The electrode-to-electrode reproducibility was also examined from the responses in 1.0 mM glucose among six different electrodes made independently following the same procedure. They showed an acceptable reproducibility with a RSD of 5.3%.

The storage stability of the glucose biosensor was performed by measuring the current response of the biosensor in pH 6.0 PBS with 1.0 mM glucose. When not in use, it was stored at 4 °C and measured at intervals. There were no obvious changes of amperometric response during the first 5 days. After storage of 15 days and a month, the biosensor retained about 95% and 85%, respectively of its original current response. Generally, there are two main factors which will affect the stability of the PB-based biosensors. One is the stability of PB in neutral solution and the other is the leakage of the enzymes. In this paper, the protect effects of SPAN and CS–GOD made PB have good stability. CS layer and 3DOM SPAN/PB structure might provide a very suitable microenvironment for GOD entrapment and retain its activity. Moreover, GA was applied to enhance the covalent bonding among SPAN, CS and GOD. These measures made the biosensor have long-time stability.

### 3.5.4. Selectivity of the glucose biosensor

The number of interfering species depends on the working potential and nature of sample. Such a low working potential of 0.0 V reduces the responses of common interferences from redox-active species that are usually present in physiological samples and improves the selectivity of glucose biosensor. Ascorbic acid (AA) and uric acid (UA) are the most common interfering electro-active species during the amperometric detection of $H_2O_2$. Hence they are also the interferents of this reported glucose biosensor which produces $H_2O_2$ in the reaction loops. There was no significant change of response current to be observed after adding AA and/or UA. The result demonstrated that the obtained biosensor had high selectivity for glucose determination, which was largely attributed to the low working potential, and the efficient and selective mediation of PB.

### 3.5.5. Human serum samples detection

To assess the performance of the glucose biosensor for real sample analysis, the concentrations of glucose in three fresh blood serum were determined by using standard addition method. The real samples were diluted to different concentrations

**Table 2**
Detection of glucose in serum samples by the proposed method and Automatic Biochemical Analyzer.

| Serum sample | Clinical assay Concentration (mM) | Proposed method ($n$ = 5) Concentration (mM) | RSD (%) |
|---|---|---|---|
| 1 | 4.80 | 4.85 | 1.04 |
| 2 | 7.40 | 7.37 | −2.70 |
| 3 | 5.90 | 5.76 | −2.37 |

(100–1000 μM) using a PBS of pH 6.0. The results are summarized in Table 2. It can be seen that the values measured by the glucose biosensor were very close to the data provided by the hospital, indicating the suitability of the proposed glucose biosensor to practical applications.

## 4. Conclusion

A novel glucose biosensor was developed on the basis of 3DOM SPAN/PB bicomponent film modified electrode. The bicomponent film was prepared by step-by-step electro-deposition via the inverted crystal template technique. PB in this 3DOM structure was stable even in weak alkaline buffer solution. The performance of the glucose biosensor has been greatly improved. The detection limit of biosensor was several orders of magnitude lower than that of other traditional PB-based glucose biosensors. The wide linear range and small $K_m$ value indicated that the 3DOM SPAN/PB film might provide a very suitable microenvironment for GOD entrapment. And the proposed biosensor had a high biological affinity toward glucose. Furthermore, the biosensor possessed satisfied stability, reproducibility and selectivity. Therefore, it can be concluded that the 3DOM SPAN/PB bicomponent film had a potential for designing various bio-electrochemical devices to provide operational access to a large group of oxidase enzymes.

## Acknowledgments

We greatly appreciate the support from the National Natural Science Foundation of China (20905035, 20805030), Youth Scientific Development Foundation of NJUT (39704002), MOE Key Laboratory of Analytical Chemistry for Life Science (KLACLS1012) and State Key Laboratory of Materials-Oriented Chemical Engineering (KL10-15). This work is also sponsored by Qing Lan Project of Education Department of Jiangsu Province.

## References

[1] J. Wang, Chem. Rev. 108 (2008) 814–825.
[2] M. Gu, J.W. Wang, Y.F. Tu, J.W. Di, Sens. Actuators B 148 (2010) 486–491.
[3] F. Ricci, G. Palleschi, Biosens. Bioelectron. 21 (2005) 389–407.
[4] M.P. O'Halloran, M. Prada, G.G. Guilbault, Talanta 55 (2001) 605–611.
[5] P. Salazar, R.K. O'Neill, M. Martín, R. Roche, J.L. González-Mora, Sens. Actuators B 152 (2011) 137–143.
[6] G.L. Fu, X.L. Yue, Z.F. Dai, Biosens. Bioelectron. 26 (2011) 3973–3976.
[7] M.H. Zhang, R. Yuan, Y.Q. Chai, W.J. Li, H.A. Zhong, C. Wang, Bioprocess Biosyst. Eng. 34 (2011) 1143–1150.
[8] Z. Wu, C.A. Tao, C.X. Lin, D.Z. Shen, G.T. Li, Chem. Eur. J. 14 (2008) 11358–11368.
[9] A. Stein, F. Li, N.R. Denny, Chem. Mater. 20 (2008) 649–666.
[10] H. Li, J.X. Wang, Z.L. Pan, L.Y. Cui, L.A. Xu, R.M. Wang, Y.L. Song, L. Jiang, J. Mater. Chem. 21 (2011) 1730–1735.
[11] A. Walcarius, A. Kuhn, TRAc—Trends Anal. Chem. 27 (2008) 593–603.
[12] D. Ramirez, P. Bartlett, M. Abdelsalam, H. Gomez, D. Lincot, Phys. Status Solidi A 205 (2008) 2365–2370.
[13] P. Bartlett, J. Baumberg, P. Birkin, M. Ghanem, M. Netti, Chem. Mater. 14 (2002) 2199–2208.
[14] P. Bartlett, M. Ghanem, I. Hallag, P. de Groot, A. Zhukov, J. Mater. Chem. 13 (2003) 2596–2602.
[15] S.H. Ding, W.P. Qian, Y. Tan, Y. Wang, Langmuir 22 (2006) 7105–7108.
[16] F. Yan, W.A. Goedel, Chem. Mater. 16 (2004) 1622–1626.
[17] X.J. Chen, J.J. Zhou, J. Xuan, W. Yan, L.P. Jiang, J.J. Zhu, Analyst 135 (2010) 2629–2636.
[18] A.A. Karyakin, E.A. Puganova, I.A. Budashov, I.N. Kurochkin, E.E. Karyakina, V.A. Levchenko, V.N. Matveyenko, S.D. Varfolomeyev, Anal. Chem. 76 (2004) 474–478.
[19] J.H.O. Owino, A. Ignaszak, A. Al-Ahmed, P.G.L. Baker, H. Alemu, J.C. Ngila, E.I. Iwuoha, Anal. Bioanal. Chem. 388 (2007) 1069–1074.
[20] D. Wang, F. Caruso, Adv. Mater. 13 (2001) 350–354.
[21] G. Subramanian, V.N. Manoharan, J.D. Thorne, D.J. Pine, Adv. Mater. 11 (1999) 1261–1265.
[22] S.N. Sawant, N. Bagkar, H. Subramanian, J.V. Yakhmi, Philos. Mag. 84 (2004) 2127–2138.
[23] Y. Sun, A.G. MacDiarmid, A.J. Epstein, Chem. Commun. 7 (1990) 529–531.
[24] Z. Wei, L. Zhang, M. Yu, Y. Yang, M. Wan, Adv. Mater. 15 (2003) 1382–1385.
[25] G. Li, Z. Zhang, Macromolecules 37 (2004) 2683–2685.
[26] C.Q. Zhang, G. Li, H.R. Peng, Mater. Lett. 63 (2009) 592–594.
[27] X.J. Chen, Z.X. Chen, J.W. Zhu, C.B. Xu, W. Yan, C. Yao, Bioelectrochemistry 82 (2011) 87–94.
[28] J. Wang, X.J. Zhang, M. Prakash, Anal. Chim. Acta 395 (1999) 11–16.
[29] F. Ricci, A. Amine, G. Palleschi, D. Moscone, Biosens. Bioelectron. 18 (2003) 165–174.
[30] X.Y. Wang, H.F. Gu, F. Yin, Y.F. Tu, Biosens. Bioelectron. 24 (2009) 1527–1530.
[31] Y.C. Luo, J.J. Xu, W. Zhao, H.Y. Chen, Sens. Actuators B 97 (2004) 249–255.
[32] H.J. Bright, M. Appleby, J. Biol. Chem. 244 (1969) 3625–3634.
[33] A.A. Karyakin, E.E. Karyakina, L. Gorton, Electrochem. Commun. 1 (1999) 78–82.
[34] L. Li, Q.L. Sheng, J.B. Zhen, H.F. Zhang, Bioelectrochemistry 74 (2008) 170–175.
[35] S. Brahim, D. Narinesingh, A. Guiseppi-Elie, Biosens. Bioelectron. 17 (2002) 53–59.
[36] C.Y. Deng, M.R. Li, Q.J. Xie, M.L. Liu, Y.M. Tan, X.H. Xu, S.Z. Yao, Anal. Chim. Acta 557 (2006) 85–94.
[37] L.D. Zhu, J.L. Zhai, Y.N. Guo, C.Y. Tian, R.L. Yang, Electroanalysis 18 (2006) 1842–1846.
[38] I.L. Mattos, M.C.C. Areias, Talanta 66 (2005) 1281–1286.
[39] A.S. Kumar, P.Y. Chen, S.H. Chien, J.M. Zen, Electroanalysis 17 (2005) 210–222.
[40] X.C. Tan, Y.X. Tian, P.X. Cai, X.Y. Zou, Anal. Bioanal. Chem. 381 (2005) 500–507.